Progress In Electromagnetics Research, Vol. 117, 339–355, 2011

ON THE ANALYTIC-NUMERIC TREATMENT OF WEAKLY SINGULAR INTEGRALS ON ARBITRARY POLYGONAL DOMAINS

S. López-Peña, A. G. Polimeridis*, and J. R. Mosig

Laboratory of Electromagnetics and Acoustics
Ecole Polytechnique Fédérale de Lausanne
Lausanne CH-1015, Switzerland

Abstract—An alternative analytical approach to calculate the weakly singular free-space static potential integral associated to uniform sources is presented. Arbitrary oriented flat polygons are considered as integration domains. The technique stands out by its mathematical simplicity and it is based on a novel integral transformation. The presented formula is equivalent to others existing in literature, being also concise and suitable within a singularity subtraction framework. Generalized Cartesian product rules built on the double exponential formula are utilized to integrate numerically the resulting analytical 2D potential integral. As a consequence, drawbacks associated to endpoint singularities in the derivative of the potential are tempered. Numerical examples within a surface integral equation-Method of Moments framework are finally provided.

1. INTRODUCTION

Surface integral equation (SIE) formulations are commonly used to solve a wide range of electromagnetic problems [1–5]. The SIE can be set either in terms of fields or in terms of potentials, calling typically in both cases for the accurate evaluation of multidimensional singular integrals. A formulation through fields magnifies this issue, since the computation of strongly singular and hypersingular integrals is required. Nevertheless, the problem is mitigated if potential formulations are utilized, since the integration of weakly singular functions is only needed.

According to the specific problem, the above-mentioned multi-dimensional weakly singular integrals can be generically tackled by

Received 31 May 2011, Accepted 10 June 2011, Scheduled 10 June 2011

* Corresponding author: Athanasios G. Polimeridis (athanasios.polymeridis@epfl.ch).

direct evaluation [6], singularity cancellation [7–9] or singularity subtraction [10–16] techniques. The last approach splits the integral into regular and weakly singular parts, which are treated separately. Numerical and analytical integration strategies are respectively employed for regular and singular terms. Interested readers could consult [6] for a more detailed survey of relevant previous work.

Static potential Green functions (GF) are inherent to the cited singular part, being the only functions to integrate in various practical situations. This is the case required when using the Method of Moments (MoM) [17] with low order basis functions to discretize the Mixed Potential Integral Equations (MPIE) [18], or when SIE-MoM strategies are utilized to tackle static problems [16]. Within a MoM framework, a Galerkin procedure invokes the static potential GF multidimensional integrals over source and observer domains, which are typically polygonal flat patches employed to mesh the surface of the objects under study. In general, a more accurate geometrical modeling of composite structures and a more efficient corresponding analysis requires different building elements, commonly triangles and quadrilaterals [19]. It is also reported that using solely quadrilateral meshing instead of triangular one could lead to a substantial reduction of the necessary number of degrees of freedom [20].

For the self-case (identical source and observer domains), the analytical expressions of the aforementioned integrals are available in literature for the most popular mesh schemes, namely triangular [12, 13] and rectangular patches [16]. More specifically, the last paper provides also the full analytical solution for several cases of interest, where source and observer rectangular domains do not intercept. Nonetheless, this is not the situation in the general case and even less for other shapes of obvious interest like quadrangles [21–23], or arbitrary polygons. Here the problem is solved by applying numerical integration techniques on the observer patch to the resulting analytical potential integral on the source patch. This strategy keeps its validity and accuracy for all the possible arrangements of source and observer domains. Of course, singularities of higher order (e.g., gradient of Green's function) call for a more elaborate treatment, as illustrated in [24].

This manuscript is devoted to the deep analysis of the prior approach. Analytical formulas to evaluate the potential integral on generic polygons have been derived in [10] through Gauss integral theorems. Basically, the surface integral is transformed into an integral over the boundary of the polygon plus a residue calculated in the neighborhood of the singularity. A related procedure is used in [11] for the specific case of the triangle, whereas the same

case is solved in [7] by utilizing some relations in [25]. Here, an alternative technique, which stands out by its mathematical simplicity, is proposed to calculate the analytical expression of the potential integral. Just like in [7, 10, 11], the technique is based on a subdomain decomposition strategy. But on the contrary, the contribution of each subdomain is analytically calculated through an, to the best of our knowledge, original transformation. It can be easily proved that the final expression presented in this paper is equivalent to those in [10, 11], being also concise and suitable for numerical integration.

In Galerkin schemes (undoubtedly the most popular version of MoM) the potential must be integrated again over the observation domain. Therefore, when source and observation domains are coincident or adjacent we are confronted with the problem of integrating a continuous function with infinite derivatives at the integration domain's boundaries. This explains why the standard (e.g., Gauss-Legendre) 2D quadratures currently available in the literature fail to produce accurate results. This drawback can be alleviated via the usage of numerical rules tailored to integrate functions with endpoint singularities, as indicated in [26, 27]. Here, these rules are applied to the previous analytical potential integral within a SIE-MoM context, and this is the second relevant contribution of this paper.

2. GEOMETRICAL CONSIDERATIONS AND ALTERNATIVE ANALYTICAL APPROACH TO EVALUATE THE POTENTIAL INTEGRAL

2.1. Statement of the Problem

The targeted 4D integral, which can appear when MoM-Galerkin schemas together with low order basis functions are utilized within singularity subtraction framework, is of the form

$$I = \int_S \int_{S'} \frac{1}{R}\, dS' dS. \tag{1}$$

In (1), S is the outer integration domain, which embraces all the observation points $\mathbf{r} = (x, y, z)$. On its turn, the source points $\mathbf{r}' = (x', y', z')$ are enclosed by the inner integration domain S'. Both domains are considered to be arbitrarily oriented flat polygonal patches, as depicted in Fig. 1. Also in (1), $1/R$ is a static potential GF (except the constant $1/4\pi\varepsilon_0$) with $R = |\mathbf{r} - \mathbf{r}'|$ the distance between observation and source points. Therefore, the inner integral in (1)

$$V = \int_{S'} \frac{1}{R}\, dS' \tag{2}$$

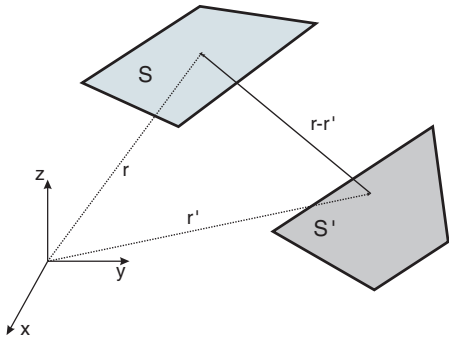

Figure 1. Arbitrarily oriented flat polygonal patches in the Cartesian frame (x, y, z), where I is performed.

physically represents the scalar potential V bounded to a uniform unit charge density distributed over a arbitrarily located flat polygonal surface S'. The boundary $\partial S'$ enclosing S' contains the N polygon's nodes $\mathbf{r'_n}$ $(n = 1 \dots N)$, which are assumed to be ordered counterclockwise with regard to the polygon surface unitary vector $\hat{\mathbf{n}}$. The value of this vector is easily generated from the nodes as $\hat{\mathbf{n}} = \mathbf{n}/|\mathbf{n}|$, being $\mathbf{n} = (\mathbf{r'_{n+1}} - \mathbf{r'_n}) \times (\mathbf{r'_{n+2}} - \mathbf{r'_{n+1}})$ with n a value between 1 and $N - 2$. An alternative analytical approach to solve (2) is presented in this manuscript and described in the next subsections.

2.2. Auxiliary Local Cartesian Frame

Commonly, the mathematical complexity of this problem is reduced by solving the problem in an auxiliary local Cartesian frame (u, v, w). Here, this frame is located at $\mathbf{r_0} = (\mathbf{r} - \hat{\mathbf{n}} \cdot c)$, with $c = (\mathbf{r} - \mathbf{r'_n}) \cdot \hat{\mathbf{n}}$ (for any n), so that $\hat{\mathbf{w}} \equiv \hat{\mathbf{n}}$ and the vectors $\hat{\mathbf{u}}$ and $\hat{\mathbf{v}}$ are within the plane $\mathscr{P}$ containing the polygon. Therefore, as exemplarily shown for a generic quadrangle in Fig. 2, within the new local frame, the point represented by $\mathbf{r}$ is confined in the w axis with coordinates $(0, 0, c)$ and any point $\mathbf{r'}$ can be expressed as $(u, v, 0)$. Consequently, the resolution of

$$V = \int_{S'} \frac{1}{\sqrt{u^2 + v^2 + c^2}} \, dS' \tag{3}$$

in this frame is equivalent to solving (2) in the original coordinate system (x, y, z). Also in Fig. 2, the vectors $\boldsymbol{\rho'_n} = \mathbf{r'_n} - \mathbf{r_0}$, lying in $\mathscr{P}$ and representing the position in the original Cartesian frame of the node $\mathbf{r'_n}$ from the origin $\mathbf{r_0}$ of the new local coordinate system, are shown.

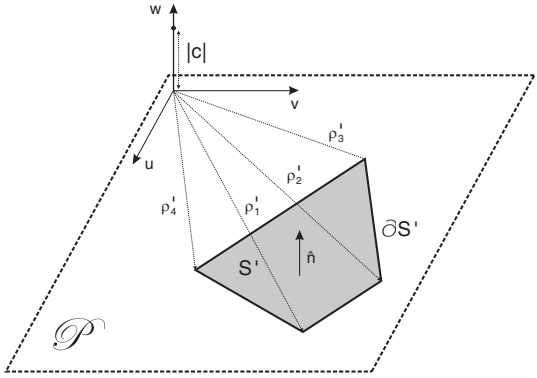

Figure 2. Main features linked to the auxiliary local Cartesian frame (u, v, w) within which the potential integral is solved.

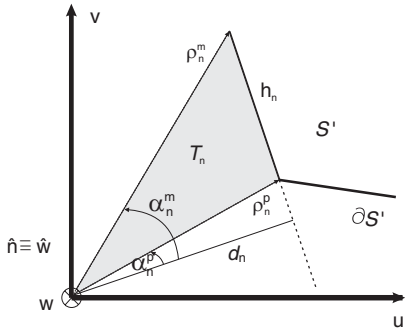

Figure 3. Geometrical description of a generic triangle T_n which is associated to the analytical resolution of V through a domain decomposition technique and a polar coordinate transformation.

2.3. Domain Decomposition Strategy

The required analytical effort to solve (3) is usually tempered through the usage of a domain decomposition technique. Namely, the integral (3) over S' is expanded as a sum of N integrals over simpler domains as

$$V = \sum_{n=1}^{N} s_n \int_{T_n} \frac{1}{\sqrt{u^2 + v^2 + c^2}}\, dS'. \tag{4}$$

These domains, denoted in (4) as T_n and described in Fig. 3, result to a set of N triangles which are enclosed by $\mathscr{P}$, whereas in [10, 11] are the edges of the polygon. It is appreciated in Fig. 3, that T_n is built

by means of the vectors $\mathbf{h}_n = \boldsymbol{\rho}_{\boldsymbol{n}}^{\boldsymbol{p}} - \boldsymbol{\rho}_{\boldsymbol{n}}^{\boldsymbol{m}}$, being $\boldsymbol{\rho}_{\boldsymbol{n}}^{\boldsymbol{m}}$ and $\boldsymbol{\rho}_{\boldsymbol{n}}^{\boldsymbol{p}}$ respectively either $\boldsymbol{\rho}'_{\boldsymbol{n}}$ and $\boldsymbol{\rho}'_{\boldsymbol{n+1}}$ for $n = 1 \ldots N-1$ or $\boldsymbol{\rho}'_{\boldsymbol{N}}$ and $\boldsymbol{\rho}'_{\boldsymbol{1}}$ for $n = N$. Also in (4), $s_n = \mathrm{sgn}(\hat{\mathbf{n}} \cdot (\boldsymbol{\rho}_{\boldsymbol{n}}^{\boldsymbol{m}} \times \boldsymbol{\rho}_{\boldsymbol{n}}^{\boldsymbol{p}}))$ is the sign of the contribution to V of each subintegral. Among the domain decomposition schemes described in the literature, this choice permits a more intuitive, simple and robust computation of the sign associated to each contribution from orthogonal vectors to the polygon. Also note, that if $\mathbf{r}$ is in a polygon edge or its extension, which is the situation where $\boldsymbol{\rho}_{\boldsymbol{n}}^{\boldsymbol{m}} || \boldsymbol{\rho}_{\boldsymbol{n}}^{\boldsymbol{p}}$, then the contribution linked to this edge vanishes.

2.4. Polar Coordinate Transformation

A close expression for (4) is only possible if its associated integrals are solved analytically. In this work, this has been done by starting with the employment of a common polar coordinate transformation, typically used in a singularity cancellation context [7]. Therefore,

$$V = \sum_{n=1}^{N} s_n \int_{\alpha_n^m}^{\alpha_n^p} \int_0^{\frac{d_n}{\cos(\alpha)}} \frac{\rho}{\sqrt{\rho^2 + c^2}} \, d\rho d\alpha \tag{5}$$

where all the involved geometric quantities can be inferred from Fig. 3 as $d_n = |\boldsymbol{\rho}_{\boldsymbol{n}}^{\boldsymbol{m}} \cdot (\hat{\mathbf{h}}_n \times \hat{\mathbf{n}})|$, $\alpha_n^m = \tan^{-1}(\boldsymbol{\rho}_{\boldsymbol{n}}^{\boldsymbol{m}} \cdot \hat{\mathbf{h}}_n / d_n)$, $\alpha_n^p = \tan^{-1}(\boldsymbol{\rho}_{\boldsymbol{n}}^{\boldsymbol{p}} \cdot \hat{\mathbf{h}}_n / d_n)$ and $\hat{\mathbf{h}}_n = \mathbf{h_n}/|\mathbf{h_n}|$.

2.5. Preliminary Analytical Processing

The first steps to solve (5) analytically are straightforward if the integral transformation $t = \rho^2 + c^2$ is employed in the inner integral. Therefore, (5) becomes

$$V = \sum_{n=1}^{N} s_n |c| \left[\int_{\alpha_n^m}^{\alpha_n^p} \sqrt{1 + \left(\frac{a_n}{\cos(\alpha)} \right)^2} \, d\alpha - \Delta\alpha_n \right] \tag{6}$$

with $\Delta\alpha_n = \alpha_n^p - \alpha_n^m$ and $a_n = d_n/|c|$.

2.6. Novel Integral Transformation and Close Form of V

This subsection is devoted to describe the analytical procedure associated to the resolution of the integral in (6). This procedure stands out by its mathematical simplicity and is based on, to the authors' knowledge, a novel integral transformation, which is of the

form

$$\gamma = \frac{\sin(\alpha)}{\sqrt{1 + \left(\frac{\cos(\alpha)}{a_n}\right)^2}}. \tag{7}$$

Expression (7) has been obtained after combining three simpler changes of variable, which allow recursively solving the integral associated to (6) in three steps. These changes are $\beta^2 = 1 + (a_n/\cos(\alpha))^2$, $\eta = \beta^2 + b$ and $\gamma = \sqrt{\eta/(\eta - b)}$, with $b = -(1 + a_n^2)$. The transformation (7) can be directly utilized in (6), so that the integrand becomes a rational function. Therefore, after a classical fraction decomposition process, (6) becomes

$$V = \sum_{n=1}^{N} s_n |c| \left[a_n \int_{\gamma_n^m}^{\gamma_n^p} \frac{d\gamma}{1-\gamma^2} + \int_{\gamma_n^m}^{\gamma_n^p} \frac{d\gamma}{a_n\left(1 + \frac{\gamma^2}{a_n^2}\right)} - \Delta\alpha_n \right] \tag{8}$$

with $\gamma_n^{(m,p)} = \sin(\alpha_n^{(m,p)})/\sqrt{1 + (\cos(\alpha_n^{(m,p)})/a_n)^2}$. The solution of the integrals appearing in (8) is really well known (2.143 in [25]) and lead to the final analytical expression for V, which is also the solution of (2),

$$\begin{aligned} V \;=\; & \sum_{n=1}^{N} s_n \Bigg\{ d_n \left(\tanh^{-1}(\gamma_n^p) - \tanh^{-1}(\gamma_n^m) \right) \\ & + |c| \left[\tan^{-1}\left(\frac{|c|\gamma_n^p}{d_n}\right) - \tan^{-1}\left(\frac{|c|\gamma_n^m}{d_n}\right) - \Delta\alpha_n \right] \Bigg\} \end{aligned} \tag{9}$$

As it has been mentioned, different analytical formulas exist in the literature for (2). The present approach, summarized in (6), (7) and (9), uses only elementary mathematics and is very well suited for being employed in numerical codes, since it is concise and easily programmable in functions of clearly identifiable geometric quantities.

2.7. Formula Validation

Here, (9) will be verified through a simple numerical experiment. This experiment is addressed to ascertain that this expression fulfils the physical properties bounded to the potential produced by a uniform charge distribution over a flat polygon. The selected source polygon is a rectangle lying on the XY plane, whose center is located at the coordinate origin. The rectangle edges, which are parallel to the coordinate axes x and y, measure respectively 0.01 along x and 1 along y. A total charge of 1 C is assumed to be distributed over the polygon surface. The observation points are $\mathbf{r_z} = (0, 0, \psi)$ and $\mathbf{r_y} = (0, \psi, 0)$,

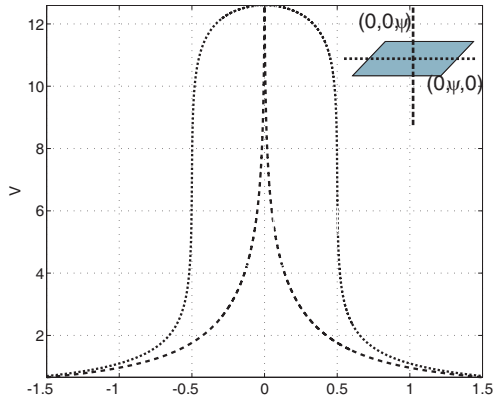

Figure 4. Resulting potentials after utilizing V for a rectangle lying on the XY plane, whose edges measure 0.01 m along x and 1 m along y. The observation points are $\mathbf{r_z} = (0, 0, \psi)$ and $\mathbf{r_y} = (0, \psi, 0)$ with $\psi = (-1.5 : 1.5)$.

being $\psi = -1.5 : 1.5$. The behavior of V on the polygon's surface S' and its boundary $\partial S'$ is checked by computing (9) on the z and y axes. The resulting potentials are represented in Fig. 4, where it can be appraised that the basic classical potential theory predictions are verified. Firstly, the potential is symmetric and continuous in both S' and $\partial S'$. Secondly, the potential's directional derivative in a direction crossing S' and parallel to $\hat{\mathbf{n}}$ will be discontinuous on S', since V exhibits an angle point at $(0, 0, 0)$ in this case. Thirdly, this derivative will be singular on $\partial S'$ in a direction lying on the plane $\mathscr{P}$ enclosing the polygon. This fact, which will be of relevance in the next section, can be inferred from Fig. 4, where the infinite value of the slope's tangents to V at $(0, -1/2, 0)$ and $(0, 1/2, 0)$ is easily intuited.

3. ON THE NUMERICAL INTEGRATION OF THE POTENTIAL DUE TO A UNIFORM CHARGE DISTRIBUTION OVER AN ARBITRARILY ORIENTED FLAT POLYGON

Doubtlessly, the Galerkin method is the most popular technique to discretize potential SIEs through the MoM. Within this framework, the use of low order basis functions together with mesh schemas compound by arbitrarily shaped polygonal patches invokes the integration of the expression (9) on the observer patch. Provided that, singularity

subtraction techniques are utilized or static problems are tackled. Typically, this integral on the observer patch is numerically performed through the employ of standard Gaussian quadratures, as for example Gauss-Legendre (GL) rules. It has to be pointed out that the abscissas of theses rules represent physically the observer points $\mathbf{r}$ enclosed by S in (1). In this section, we demonstrate a new approach for overcoming the inaccuracy linked to the usage of GL quadratures, after analyzing by analytical means the source of the problem.

As empirically inferred from Fig. 4, the derivatives of expression (9) will exhibit endpoint singularities on $\partial S'$ in a direction lying on the plane $\mathscr{P}$ housing the polygon. As aforementioned, this fact is totally coherent with classical potential theory, considering that these derivatives are connected to the electric field in $\mathscr{P}$, which is produced by a uniform surface charge distribution confined within a polygon, being this field singular in the polygon boundary. In the enhancement of the numerical integration of (9), it is crucial to have a good knowledge of the analytical features inherent to the singularity which is being faced. This objective can be easily attained through the study of the potential in the plane confining the polygon, which results to the expression (9) for $c = 0$. In this case, the employ of the identity $\sin(\tan^{-1}(\tau)) = \tau/\sqrt{1+\tau^2}$ leads to $\gamma_n^{(m,p)}|_{c=0} = \boldsymbol{\rho}_n^{(m,p)} \cdot \hat{\mathbf{h}}_n / |\boldsymbol{\rho}_n^{(m,p)}|$, with $|\boldsymbol{\rho}_n^{(m,p)}| = \sqrt{d_n^2 + (\boldsymbol{\rho}_n^{(m,p)} \cdot \hat{\mathbf{h}}_n)^2}$, easily deduced from Fig. 3. Consequently, after some basic algebraic manipulations, (9) for $c = 0$ can be now expressed as

$$V_0 = \sum_{n=1}^{N} s_n \left[d_n \ln\left(A_n^p A_n^m\right) - 2 d_n \ln\left(d_n\right) \right] \tag{10}$$

where $A_n^p = (|\boldsymbol{\rho}_n^p| + \boldsymbol{\rho}_n^p \cdot \hat{\mathbf{h}}_n)$ and $A_n^m = (|\boldsymbol{\rho}_n^m| - \boldsymbol{\rho}_n^m \cdot \hat{\mathbf{h}}_n)$. Direct inspection of (10) clearly reveals that, for any extension, an endpoint singular behavior is produced by $d_n \ln(d_n)$ in the directional derivative $\partial V_0 / \partial d_n$ when $d_n \to 0$ (i.e., for $\mathbf{r}$ in $\mathscr{P}$ and tending to $\partial S'$). This endpoint logarithmic singularity can be explicitly appraised in the expression of the electric field $\mathbf{E_0}$ produced by a polygonal uniform charge distribution when $c = 0$, which invokes the calculation of the gradient of (10). The analytical expression of this field is

$$\mathbf{E_0} = \sum_{n=1}^{N} s_n \left\{ 2\mathbf{D_n^d} \left[\ln\left(d_n\right) - \ln\left(\sqrt{A_n^m A_n^p} \right) + 1 \right] - d_n \left[\frac{\mathbf{D_n^p}}{A_n^p} + \frac{\mathbf{D_n^m}}{A_n^m} \right] \right\} \tag{11}$$

where $\mathbf{D_n^p} = -(\hat{\mathbf{h}} + \boldsymbol{\rho}_n^p / |\boldsymbol{\rho}_n^p|)$, $\mathbf{D_n^m} = (\hat{\mathbf{h}} - \boldsymbol{\rho}_n^m / |\boldsymbol{\rho}_n^m|)$ and $\mathbf{D_n^d} = -\mathrm{sgn}(\boldsymbol{\rho}_n^m \cdot (\hat{\mathbf{h}}_n \times \hat{\mathbf{n}}))(\hat{\mathbf{h}}_n \times \hat{\mathbf{n}})$. In Fig. 5, the singular behavior of

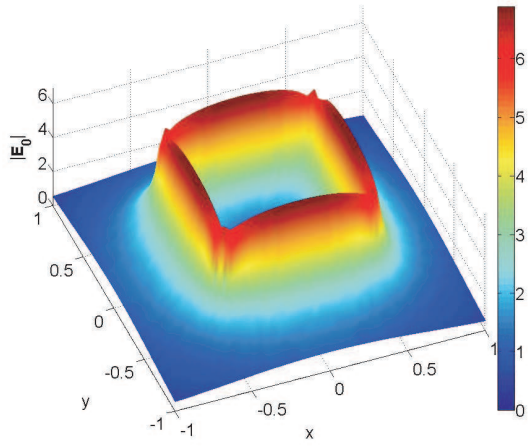

Figure 5. Computed electric field magnitude in the XY plane for a charge density uniformly distributed on a 1 m edge square, which lies in the XY plane and is centered at the origin.

(11) is illustrated through the representation of $|\mathbf{E_0}|$ produced by a $\sigma = 1\,\mathrm{C/m^2}$ surface charge density, which is uniformly distributed over a 1 m edge square, which lies in the XY plane and is centered at the origin. It has to be pointed the irrelevance of the shape of these boundaries. Namely, the same sort of singular behavior is expected for a polygonal contour, whose number of edges is either finite or, in the limiting case, infinite, as for instance a circumference or a curved patch. This fact is obvious when the singular behavior obtained in (11) is compared with the classical analytical solution giving the electrostatic field created by a uniformly charged disk on its edge [28]. Therefore, it can be concluded that mesh schemas based on curved contour patches [29] are not devoid of the inconveniences caused by these endpoint singularities.

As aforesaid and illustrated in (1), a Galerkin schema within a MoM framework can invoke the computation of the integral of (9) over the observer domain. According to the relative position of this domain with regard to the source patch, the integration scenarios of interest, in which the singular behavior in the derivatives of (9) is enhanced, can be classified as weakly singular or near singular. On the one hand, weakly singular situations appear when source and observer domains are the same or share an edge or a vertex. On the other hand, near singular cases arise when source and observer cells are very close but

their boundaries are totally separated.

Gaussian quadratures are tailored to numerically integrate smooth functions, namely, continuous functions with continuous derivatives. This is not the case in the above-mentioned situations, where the terms $d_n \ln(d_n)$ of the integrand magnify the logarithmic endpoint singular behavior of the integrand's derivatives in the patch boundary. Functions exhibiting this type of singularity are accurately integrated by means of the double exponential (DE) quadrature formula, as demonstrated in [26]. On its turn, [27] evinces that generalized Cartesian product rules, based on this formula, outperform Gaussian rules for some situations of interest. These situations are, weakly singular scenarios related either to coincident or to adjacent orthogonal domains and the near singular case associated to very close parallel cells.

In this manuscript, the weakly singular cases related to coplanar domains sharing an edge or a vertex are presented. These situations appear in most of the mesh schemas linked to planar of faceted structures. This study is performed, without loss of generality, through the employ of square source and observer patches. The source patch's nodes are $\mathbf{r'_1} = (1/2, -1/2, 0)$, $\mathbf{r'_2} = (1/2, 1/2, 0)$, $\mathbf{r'_3} = (-1/2, 1/2, 0)$ and $\mathbf{r'_4} = (-1/2, -1/2, 0)$, whereas the observer patches are set by $\mathbf{r_1} = (1/2, 1/2, 0)$, $\mathbf{r_2} = (1/2, 3/2, 0)$, $\mathbf{r_3} = (-1/2, 3/2, 0)$, $\mathbf{r_4} = (-1/2, 1/2, 0)$, for the adjacent case, and $\mathbf{r_1} = (-1/2, 1/2, 0)$, $\mathbf{r_2} = (-1/2, 3/2, 0)$, $\mathbf{r_3} = (-3/2, 3/2, 0)$, $\mathbf{r_4} = (-3/2, 1/2, 0)$ for the common vertex situation. Fig. 6 and Fig. 7 show respectively for adjacent and common vertex cases, the relative error when calculating the source integral through (9) and the observer integral by means of generalized 2D Cartesian product rules based either on the DE formula or on the Gauss-Legendre rules. The reference solutions of the 4D integrals are computed by utilizing the analytical expressions in [16]. The cubature levels for the numerical integration are defined as in [27], corresponding levels 0, 1, 2, 3, and 4 respectively to 7, 13, 25, 51 and 101 integration points per dimension. It can be appreciated in Fig. 6, that DE based rules outperform the Gaussian schemes for the adjacent case, whereas Fig. 7 exhibit that both numerical integration strategies are equivalent for the common vertex situation. This occurs because, in the last case, most of the observer domain is located in a smooth variation region of the fields, so that the potential can be accurately integrated through Gaussian rules. On the contrary, in the adjacent situation, the observation patch includes a substantial part of the singular region of the fields. Consequently, Gaussian rules lose their accuracy in favor of DE based rules, which are tailored to work in this endpoint singular region of the potential derivatives.

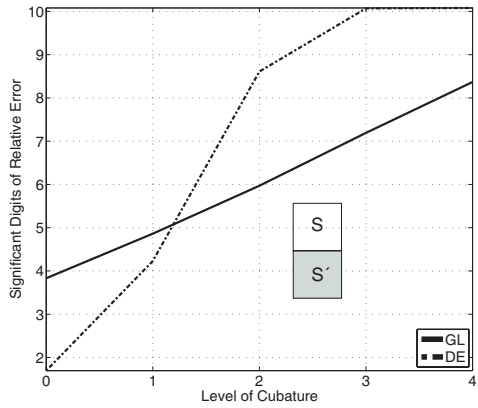

Figure 6. Relative error in calculating the 4D adjacent case weakly singular integral utilizing V together with a 2D generalized Cartesian product rule based on the DE formula and Gauss-Legendre quadrature rules. Source cell nodes are $\mathbf{r'_1} = (1/2, -1/2, 0)$, $\mathbf{r'_2} = (1/2, 1/2, 0)$, $\mathbf{r'_3} = (-1/2, 1/2, 0)$ and $\mathbf{r'_4} = (-1/2, -1/2, 0)$, whereas observer cell vertices are $\mathbf{r_1} = (1/2, 1/2, 0)$, $\mathbf{r_2} = (1/2, 3/2, 0)$, $\mathbf{r_3} = (-1/2, 3/2, 0)$ and $\mathbf{r_4} = (-1/2, 1/2, 0)$.

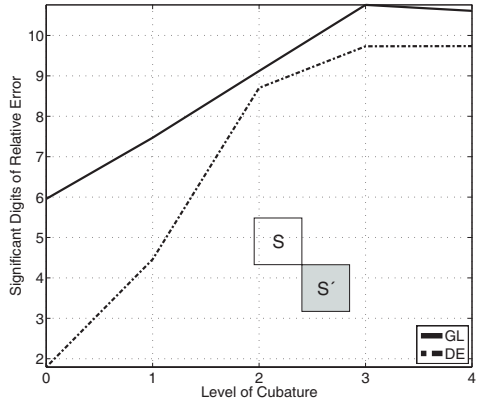

Figure 7. Relative error in calculating the 4D adjacent case weakly singular integral utilizing V together with a 2D generalized Cartesian product rule based on the DE formula and Gauss-Legendre quadrature rules. Source cell nodes are $\mathbf{r'_1} = (1/2, -1/2, 0)$, $\mathbf{r'_2} = (1/2, 1/2, 0)$, $\mathbf{r'_3} = (-1/2, 1/2, 0)$ and $\mathbf{r'_4} = (-1/2, -1/2, 0)$, whereas observer cell vertices are $\mathbf{r_1} = (-1/2, 1/2, 0)$, $\mathbf{r_2} = (-1/2, 3/2, 0)$, $\mathbf{r_3} = (-3/2, 3/2, 0)$ and $\mathbf{r_4} = (-3/2, 1/2, 0)$.

4. NUMERICAL EXAMPLE

As aforementioned, the formulation presented here is useful to compute the MoM matrix elements through a singularity subtraction strategy. Basically, this strategy consists of extracting a static problem from a complete full-wave problem. Namely, the GF static part, which includes the GF spatial singular behavior, is separated from the GF dynamic part and processed severally. Consequently, the computation of a static MoM impedance matrix is invoked. Therefore, it can be concluded that a good knowledge of the static interactions in the structures under study is mandatory, since they are not only relevant for the zero frequency case; otherwise they play a very important role in the whole spectrum.

This section is devoted to show the worthiness of using 2D Cartesian product rules based on DE formula to integrate potentials as (9) to compute the Galerkin-MoM matrix static interactions within a SIE-MoM framework. The resolution of a very simple static problem is only required to achieve the objective. This problem consists of computing the total charge of a trapezohedron at 1 V from the induced charge on its surface. The inset in Fig. 8 shows the 3D trapezohedron,

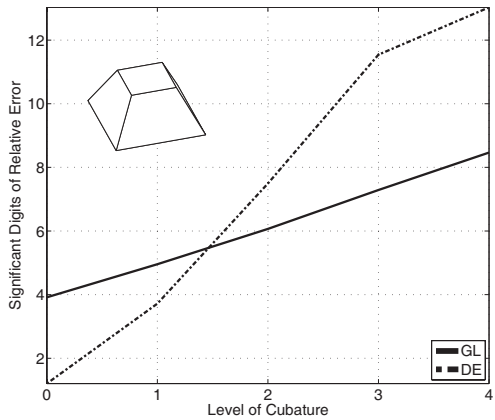

Figure 8. Relative error in calculating the total charge in a trapezohedron at 1 V. Trapezohedron's bottom and top sides are parallel squares separated by 0.5 m and centered at z axis. The squares' edges measure respectively 1 m for the bottom side and 0.5 m for the top one. The SIE (12) is discretized through the MoM, whose associated matrix is computed by means of V together with a 2D generalized Cartesian product rule based either on the DE formula or on the Gauss-Legendre quadrature rule.

whose bottom and top sides are parallel squares, which separated by 0.5 m and centered at z axis. The lengths of the squares' edges are respectively 1 m for the bottom side and 0.5 m for the top one. The SIE to solve is

$$\int_{S'} \frac{\sigma_{S'} dS'}{R} = 1 \tag{12}$$

where S' is the surface of the trapezohedron and $\sigma_{S'}$ the surface charge density, which is expanded by means of uniform basis functions on each cell. All the needed MoM matrix integrals are related to the weakly and near singular interactions previously described. It has to be pointed out that the static MoM matrix, which is associated to the MPIE full-wave analysis of the same structure, can be built from the MoM matrix required here, if low order basis functions are used [18]. These matrix elements are computed by integrating (9) through 2D generalized Cartesian product rules based on the DE and Gauss-Legendre rules, for levels 0, 1, 2, 3 and 4 in both cases. The relative errors in the resulting total charge are shown in Fig. 8. The reference solution for this error is also computed though 2D generalized Cartesian product rules based on the DE quadrature with level 6 (405 points per dimension). It can be clearly appraised in Fig. 8, that the joint use of (9) and DE-based rules outperform Gaussian rules within a complete SIE-MoM framework.

5. CONCLUSION

A novel integral transformation is presented for the analytical calculation of the weakly singular free space static potential integrals associated to uniform sources distributed over arbitrarily shaped flat polygons. When compared with other existing techniques, this transformation eases considerably the mathematical effort and provides a concise, operative and accurate framework to the singularity subtraction procedures. The equivalency between the obtained expression with this alternative strategy and other existing formulas can be proven. Numerical integration drawbacks, bounded to the endpoints singularities in the derivatives of the analytical potential integral, are alleviated through the usage of generalized Cartesian product rules based on the DE formula. Numerical examples showing these aspects are presented within a SIE-MoM framework, demonstrating the interest of using the global approach presented in this paper for the double surface integrals appearing in Galerkin formulations.

REFERENCES

1. Araújo, M. G., J. M. Taboada, F. Obelleiro, J. M. Bértolo, L. Landesa, J. Rivero, and J. L. Rodriguez, "Supercomputer aware approach for the solution of challenging electromagnetic problems," *Progress In Electromagnetics Research*, Vol. 101, 241–256, 2010.
2. Taboada, J. M., M. G. Araújo, J. M. Bértolo, L. Landesa, F. Obelleiro, and J. L. Rodriguez, "MLFMA-FFT parallel algorithm for the solution of large-scale problems in electromagnetics," *Progress In Electromagnetics Research*, Vol. 105, 15–30, 2010.
3. Ergül, Ö., T. Malas, and L. Gürel, "Solutions of large-scale electromagnetics problems using an iterative inner-outer scheme with ordinary and approximate multilevel fast multipole algorithms," *Progress In Electromagnetics Research*, Vol. 106, 203–223, 2010.
4. Shi, Y., X. Luan, J. Qin, C. J. Lv, and C. H. Liang, "Multilevel Green's function interpolation method solution of volume/surface integral equation for mixed conducting/bi-isotropic objects," *Progress In Electromagnetics Research*, Vol. 107, 239–252, 2010.
5. Chen, Y., S. Yang, S. He, and Z. Nie, "Fast analysis of microstrip antennas over a frequency band using an accurate MoM matrix interpolation technique," *Progress In Electromagnetics Research*, Vol. 109, 301–324, 2010.
6. Polimeridis, A. G. and T. V. Yioultsis, "On the direct evaluation of weakly singular integrals in Galerkin mixed potential integral equation formulations," *IEEE Trans. Antennas and Propagat.*, Vol. 56, 3011–3019, 2008.
7. Rossi, L. and P. J. Cullen, "On the fully numerical evaluation of the linear-shape function times the 3-D Green's function on a plane triangle," *IEEE Trans. Microw. Theory Tech.*, Vol. 47, 398–402, 1999.
8. Khayat, M. A. and D. R. Wilton, "Numerical evaluation of singular and near-singular potential integrals," *IEEE Trans. Antennas and Propagat.*, Vol. 53, 3180–3190, 2005.
9. Graglia, R. D. and G. Lombardi, "Machine precision evaluation of singular and nearly singular potential integrals by use of Gauss quadrature formulas for rational functions," *IEEE Trans. Antennas and Propagat.*, Vol. 56, 981–998, 2008.
10. Wilton, D. R., S. M. Rao, A. W. Glisson, D. H. Schaubert, O. M. AL-Bundak, and C. M. Butler, "Potential integrals for uniform and linear source distributions on polygonal and

polyhedral domains," *IEEE Trans. Antennas and Propagat.*, Vol. 32, 276–281, 1984.

11. Graglia, R. D., "On the numerical integration of the linear shape functions times the 3-D Green's function or its gradient on a plane triangle," *IEEE Trans. Antennas and Propagat.*, Vol. 41, 1448–1455, 1993.
12. Eibert, T. F. and V. Hansen, "On the calculation of potential integrals for linear source distributions on triangular domains," *IEEE Trans. Antennas and Propagat.*, Vol. 43, 1499–1502, 1995.
13. Arcioni, P., M. Bressan, and L. Perregrini, "On the evaluation of the double surface integrals arising in the application of the boundary integral method to 3-D problems," *IEEE Trans. Microw. Theory Tech.*, Vol. 45, 436–439, 1997.
14. Järvenpää, S., M. Taskinen, and P. Ylä-Oijala, "Singularity subtraction technique for high-order polynomial vector basis functions on planar triangles," *IEEE Trans. Antennas and Propagat.*, Vol. 54, 42–49, 2006.
15. Asvestas, J. S. and H. J. Bilow, "Line-integral approach to computing impedance matrix elements," *IEEE Trans. Antennas and Propagat.*, Vol. 55, 2767–2772, 2007.
16. López-Peña, S. and J. R. Mosig, "Analytical evaluation of the quadruple static potential integrals on rectangular domains to solve 3-D electromagnetic problems," *IEEE Trans. Magn.*, Vol. 54, 1320–1323, 2009.
17. Harrington, R. F., *Field Computation by Moment Methods*, Macmillan, New York, FL, Krieger, 1983.
18. Mosig, J. R., "Arbitrarily shaped microstrip structures and their analysis with a mixed potential integral equation," *IEEE Trans. Microw. Theory Tech.*, Vol. 36, 314–323, 1988.
19. Kolundzija, B. M. and A. R. Djordjevic, *Electromagnetic Modeling of Composite Metallic and Dielectric Structures*, Artech House, Norwood, MA, USA, 2002.
20. Kolundzija, B. M., M. M. Kostic, B. L. Mrdakovic, and D. S. Sumic, "Comparison of different strategies for conversion of triangular mesh into quadrilateral mesh," *EuCAP 2010 — The 4th European Conference on Antennas and Propagation*, 2010.
21. Adams, T. and J. Singh, "A nonrectangular patch model for scattering from surfaces," *IEEE Trans. Antennas and Propagat.*, Vol. 27, 531–535, 1979.
22. Tulyathan, P. and E. H. Newman, "A surface patch model for polygonal plates," *IEEE Trans. Antennas and Propagat.*, Vol. 30,

588–593, 1982.

23. Kolundzija, B. M., "On the locally continuous formulation of surface doublets," *IEEE Trans. Antennas and Propagat.*, Vol. 46, 1879–1883, 1998.
24. Gürel, L. and Ö. Ergül, "Singularity of the magnetic-field integral equation and its extraction," *IEEE Antennas Wireless Propag. Lett.*, Vol. 4, 229–232, 2005.
25. Gradshteyn, I. S. and I. M. Ryzhik, *Tables of Integrals, Series and Products*, Academic, New York, 1980.
26. Bailey, D. H., K. Jeyabalan, and X. S. Li, "A comparison of three high-precision quadrature schemes," *Experimental Mathematics*, Vol. 3, 317–329, 2005.
27. Polimeridis, A. G. and J. R. Mosig, "Evaluation of weakly singular integrals via generalized Cartesian product rules based on the double exponential formula," *IEEE Trans. Antennas and Propagat.*, Vol. 58, 1980–1988, 2010.
28. Durand, E., *Electrostatique: I. Les Distributions*, Masson, Paris, 1964.
29. Notaros, B. M., "Higher order frequency-domain computational electromagnetics," *IEEE Trans. Antennas and Propagat.*, Vol. 56, 2251–2276, 2008.